



**Politecnico  
di Torino**



**Maynooth  
University**  
National University  
of Ireland Maynooth



## **Small scale WEC rig for control demonstration**

### **Master degree in Mechatronic Engineering**

Politecnico di Torino

September 2023

#### *Supervisors*

Dr. Giuseppe Giorgi  
Prof. John Ringwood  
Dr. Nicolás Faedo  
MSc. Edoardo Pasta

#### *Candidate*

Dr. Jacopo Ramello



# Abstract

Control systems are ubiquitous in modern life, infusing an enormous variety of systems with performance enhancement, crossing many discipline areas. Control systems can have a variety of functions, designed to improve and enhance system behaviour, operability, safety and performance.

Renewable energy systems, which form an important pillar in climate action, can benefit from control system technology in improving energy output delivery, making such system more economic. In particular, wave energy is struggling with economic viability, compared to other renewable and non-renewable energy sources, and effective control system have been shown to increase energy capture by a factor of 2-3.

This thesis documents a study developing a small-scale wave tank, containing an operating wave energy converter (WEC) with active control, the first such demonstration of electronic WEC control at this scale (1/100). The full demonstration system cost just €500, including tank, wavemaker, etc and this thesis provides full details concerning system construction, specification, testing and performance, as well as aspects related to demonstration appeal.

The experimental setup can serve as a valuable resource for introductory research inquiries, catering to both high school and university-level studies. This accessibility opens doors for a broader audience to engage with the potential of this promising technology.



# Acknowledgments

As a conclusion of this university experience, I would like to thank my parents firstly, for giving me this opportunity and sustaining me. Then, my brothers, who are always a good reason to come back home, and all my relatives for their unconditional love.

For my last academic path, my supervisor Giuseppe, who helped me and guided me during the thesis, Professor John for the tremendous support in the development of this project, both academically and personally, as a very friendly person, Iain, John Maloco, and Tom Kelly for the significant advice and the time they dedicated to me, and Carrie for making my Irish life much easier. The entire COERlab team made my days in Ireland always fun and amazing. Thanks to all my old friends for always being there and to all the university ones for making these years in Turin very enjoyable.

Finally, thanks to my flatmates, both the past ones and the current ones, for making me feel at home whenever I was in the house.

It has been the best journey!



# Detailed Contents

<b>Abstract</b>	<b>iii</b>
<b>Acknowledgments</b>	<b>v</b>
<b>Detailed Contents</b>	<b>vii</b>
<b>List of Acronyms</b>	<b>ix</b>
<b>1 Design consideration</b>	<b>1</b>
1.1 Type of WEC inspected . . . . .	1
1.1.1 Attenuator . . . . .	2
1.1.2 Flap . . . . .	2
1.1.3 Oscillating Water Column . . . . .	3
1.1.4 Point Absorber . . . . .	4
1.2 Control strategy inspected . . . . .	5
1.2.1 Resistive loading control . . . . .	6
1.2.2 Reactive control . . . . .	7
1.2.3 Latching control . . . . .	7
<b>2 Construction and specification</b>	<b>10</b>
2.1 Hardware . . . . .	10
2.1.1 Tank . . . . .	11
2.1.2 Beach . . . . .	11
2.1.3 Wave generator . . . . .	12
2.1.4 WEC . . . . .	13
2.1.5 Micro controller and electronic . . . . .	15
2.1.6 Wave probe . . . . .	16
2.2 Software and control strategy . . . . .	17
2.2.1 Modified latching . . . . .	17
2.3 Rig pictures . . . . .	19
<b>3 Test and results</b>	<b>21</b>
3.1 Wave fidelity . . . . .	21
3.2 Phase regulation . . . . .	23
3.3 Power increase . . . . .	24

<b>4 Conclusion</b>	<b>26</b>
<b>Bibliography</b>	<b>27</b>

# List of Acronyms

## D

**DoF** Degree of Freedom.

## L

**LCOE** Levelised Cost of Energy.

## O

**OB** Oscillating Body.

**OWC** Oscillating Water Column.

## P

**PI** Proportional-Integral.

**PP** Peak-to-peak.

**PTO** Power Take Off.

## S

**SWL** Still Water Level.

## W

**WEC** Wave Energy Converter.



## Contents of this chapter

---

1.1	Type of WEC inspected . . . . .	1
1.1.1	Attenuator . . . . .	2
1.1.2	Flap . . . . .	2
1.1.3	Oscillating Water Column . . . . .	3
1.1.4	Point Absorber . . . . .	4
1.2	Control strategy inspected . . . . .	5
1.2.1	Resistive loading control . . . . .	6
1.2.2	Reactive control . . . . .	7
1.2.3	Latching control . . . . .	7

---

In pursuit of the established objectives, the attention is directed towards the systematic design of every component within the system.

A modular design approach is adopted to facilitate the seamless interchangeability of individual parts, thereby accommodating scenarios such as malfunction, enhancements, or the evaluation of alternative devices.

Opting for press-fit connections over conventional fastening methods such as screws or adhesive ensures streamlined assembly and disassembly processes, diminishing the likelihood of leakage or structural compromise attributed to perforations.

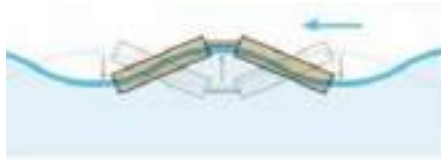
Leveraging 3D drawing software, specifically OnShape, has proven to be an indispensable asset in visualizing and ensuring the accurate assembly of components. Additionally, this tool facilitates effortless project sharing, promoting reproducibility and accessibility for others interested in replicating the design.

## 1.1 Type of WEC inspected

A survey encompassing some WECs was conducted to ascertain the optimal type that aligns with the intended purpose.

### 1.1.1 Attenuator

The configuration adopted for the Attenuator capitalizes on the relative motion between two or more interconnected legs. These segments are interconnected through hinges, and the generator body is attached to one segment while the shaft is affixed to another [1].



A fundamental requirement of this device is its buoyancy atop the water surface, thereby presenting a significant challenge to ensure effective water sealing for the electronic components. Moreover, achieving a perceptible visual distinction between controlled and uncontrolled motion necessitates a substantial wave height to ensure demonstrative experimental outcomes [1].

Even if probably possible to implement, for those two reasons this solution has been discarded, considering the small amplitude achievable in the tank and the addition of the problem of possible infiltration of water inside the device.

### 1.1.2 Flap

The Flap type operates by harnessing the circular motion of water particles through the controlled motion of submerged or semi-submerged panels or flaps.



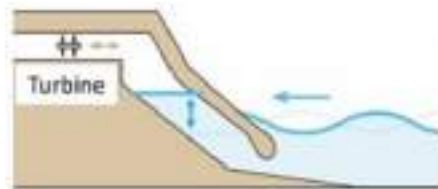
As incident waves interact with these panels, they induce oscillatory pitching or heaving motions, leading to relative movement between the panels and their fixed supports. This relative motion is then translated into mechanical energy through innovative linkages and hydraulic systems. The mechanical energy is subsequently converted into usable electrical power using generators or hydraulic pumps [2].

Once more, the waterproof sealing of electronic components becomes a pivotal concern, considering also the pressure increase due to the

water column above. Even considering a reversed architecture with the flap hold in place by a structure above, the hardware became more complicated, especially for control purposes, requiring a controllable PTO for both power absorption and delivery and Real-time computation to solve the nonlinear control optimization algorithm [3]. For those reasons this solution has been discard.

### 1.1.3 Oscillating Water Column

The Oscillating Water Column operates on the principle of exploiting the oscillatory motion of air within a chamber caused by the rise and fall of waves. As waves approach the chamber, the water level inside rises, compressing the trapped air. Subsequent wave recession leads to the expansion of the trapped air, resulting in a cyclical movement of air in and out of the chamber. This alternating airflow drives a turbine connected to a generator, thus converting the kinetic energy of the oscillating air column into usable electrical power [1].

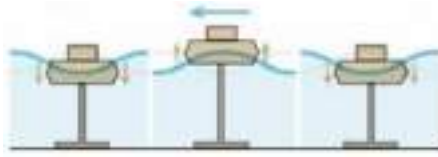


In this scenario, the electronic components can be maintained in a dry environment, considerably simplifying the implementation process. However, this advantage is accompanied by certain challenges. The intricate interplay among waves, air dynamics, air-turbine interactions, and their interaction with the chamber introduces a highly complex hydrodynamic model, essential for the effective deployment of a control algorithm governing the turbine's operation. This complexity is further exacerbated by magnified frictional and viscous forces attributed to the system's reduced scale [1].

For such a small scale a precise modelling of the system results almost impossible, leading to the impossibility of a precise control strategy.

### 1.1.4 Point Absorber

The Point Absorber operates on the principle of exploiting the vertical oscillations of a buoyant structure that is tethered to the seabed. As ocean waves propagate, they impart a cyclical upward and downward movement to the buoyant device.



This oscillatory motion is transmitted through the mooring system to a PTO mechanism, such as a hydraulic pump or an electrical generator. The conversion of the buoy's kinetic energy into usable electrical power occurs through the reciprocating motion of the PTO mechanism [1][2].

In our specific context, a deviation from the conventional approach involves employing a gantry system to secure the buoy, circumventing the need for mooring to the tank bottom. This strategic modification ensures the complete isolation of electronic components from water, ensuring a dry environment, while also confining the buoy's motion to a single degree of freedom, thereby simplifying the system dynamics while maintaining real condition fidelity. This novel configuration presents distinct advantages. Furthermore, the introduction of various control techniques is feasible, and their efficacy is readily discernible through observed amplitude variations. The operational requirements of the buoy are not contingent on exceptionally high wave conditions, and the inherent natural resonance frequency can be readily tailored by adjusting factors such as mass or buoyancy. Taking into account all of these considerations this configuration is chosen to be the most feasible.

In order to have a deeper knowledge of the system and to perform the tuning of the Automatic Control a model is required.

The WEC is subjected to various external forces during its operation. These forces include the excitation force from the waves  $f_{ex}(t)$  and the control force generated by the PTO  $f_u(t)$ , representing the primary forces. Additionally, hydrodynamic and hydro-static forces come into play as consequences of the device's motion in the water. These forces encompass the radiation force  $f_r(t)$ , diffraction force  $f_d(t)$ , viscous damping force  $f_v(t)$ , and buoyancy force  $f_b(t)$  [.]

The radiation force  $f_r(t)$  acts as a damping and inertial force, emerging because the motion of the device, which generates radiated waves, is influenced by the surrounding fluid. Notably, radiation forces persist even in the absence of incident waves and can be estimated through free response tests. In contrast, the diffraction force  $f_d(t)$  characterizes the force experienced by the device when it scatters incident waves, and it remains independent of the device's motion.

The viscous damping force  $f_v(t)$  is a nonlinear force that becomes significant as the device's velocity increases. It becomes particularly relevant when the device's surface features discontinuities, such as flanges, leading to the formation of vortices. Lastly, the buoyancy force  $f_b(t)$  results from the deviation of the device from its equilibrium (still water) position. It represents a balance between the Archimedes buoyancy force and the force of gravity [4].

We can say that equation of motion, following Newton's second law and where a superposition of forces is assumed [4], in 1 DOF is

$$M\dot{v}(t) = f_{ex}(t) + f_m(t) + f_r(t) + f_d(t) + f_v(t) + f_b(t) + f_u(t) \quad (1.1)$$

## 1.2 Control strategy inspected

The control of a WEC is intrinsically complex, as it seeks to optimize energy extraction from an irregular oscillatory motion. Modeling a WEC presents considerable challenges too due to its characteristics as a solid body floating on water, giving rise to intricate hydrodynamic interactions. The base of control can be found the energy maximization problem by considering the force-to-velocity model of a WEC, which is obtained in the frequency domain as

$$\frac{V(\omega)}{F_{ex}(\omega) + F_u(\omega)} = \frac{1}{Z_i(\omega)} \quad (1.2)$$

where  $Z_i(\omega)$  is termed the intrinsic impedance of the system and  $V(\omega)$ ,  $F_{ex}(\omega)$  and  $F_u(\omega)$  represent the Fourier transform of the velocity  $v(t)$ , excitation force  $f_{ex}(t)$  and control force  $f_{PTO}(t)$ , respectively.

The model in (1.2)[4] allows the derivation of conditions for optimal energy absorption and the intuitive design of the energy-maximizing

controller in the frequency domain as

$$Z_{PTO}(\omega) = Z_i^*(\omega) \quad (1.3)$$

where  $()^*$  denotes the complex conjugate. The choice of  $Z_{PTO}(\omega)$  as in (1.3) is referred to as complex conjugate control.

The condition in (1.3)[4] can alternatively be expressed in terms of an optimal velocity profile as

$$V^{OPT}(\omega) = \frac{F_{ex}(\omega)}{2R_i(\omega)} \quad (1.4)$$

where  $R_i = 1/2(Z_i + Z_i^*)$  is the real part of  $Z_i$ . The condition in (1.4) is a condition on the amplitude of  $V^{OPT}(\omega)$ , with the restriction that  $V^{OPT}(t)$  be in phase with  $f_{ex}(t)$ , since  $R_i(\omega)$  is a real (and even) function.

Over the course of time, an array of control strategies has been conceived and refined for Point Absorber. These strategies span a spectrum from intricate and potent methodologies, exemplified by the Model Predictive Control (MPC)[1], to more simple and sometimes less effective alternatives.

A survey of the available strategies has been conducted, guided by the quest for an optimal balance between feasibility and the realization of defined objectives. As a result of this evaluation, the spotlight has converged on three specific control strategies that exhibit a judicious compromise between practical implementability and the attainment of designated goals.

### 1.2.1 Resistive loading control

Passive damping control is trying to accomplish both the phase and amplitude requirements as explained in equation (1.4). It is considered to be a sub-optimal control due to the possibility to influence just the damping of the system and not to accelerate it [4].

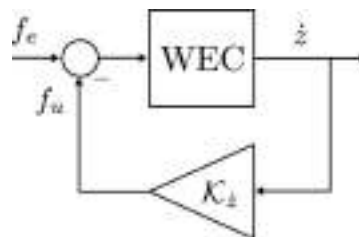


Figure 1.1: Control scheme

This alignment is achieved by incorporating a gain factor into the instantaneous velocity [5], thereby influencing power absorption and facilitating controlled deceleration of the device as in Figure 1.1. Successful implementation of passive damping necessitates a tunable PTO system capable of precise power absorption, as well as an accurate measure or estimation of the instantaneous velocity for effective feedback control.

$$f_u = B_1 \dot{z}, \quad (1.5)$$

### 1.2.2 Reactive control

Reactive control techniques strive to accomplish the entire impedance matching requirement, as in equation (1.3)[4], by introducing gains to both the velocity and position of the device [5], as in Figure 1.2, fulfilling both the phase and amplitude requirements as in equation (1.4)[6].

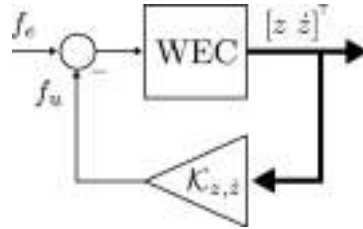


Figure 1.2: Control scheme

In this context, the PTO system is required to exert a force on the buoy, enabling acceleration or tuning of power absorption to achieve damping. Effective application of this technique mandates accurate measurements or estimations of both buoy instantaneous velocity and position and wave excitation force.

$$f_u = K_2 z + B_2 \dot{z}, \quad (1.6)$$

### 1.2.3 Latching control

Latching control is implemented to satisfy just the phase matching condition, as can be seen in equation (1.4)[4], by synchronizing the velocity of the device with the excitation force of the incoming wave. This strategy involves halting the buoy's motion, or latching it, when its velocity reaches zero for a certain duration, subsequently releasing it [5]. Accurate computation of the latching time is crucial and requires precision, determined by analyzing the wave spectrum and predicting

the wave profile. This technique ensures that the device attains optimal phase alignment with the wave-induced motion, thus enhancing its overall energy capture efficiency.

Notably, for sine waves of specific frequencies, the latching time can be computed offline and remains constant.

The hardware requisites encompass a simple mechanism akin to an "handbrake" to immobilize the device [4]. Although the mechanism may appear deceptively straightforward, it constitutes one of the control actions that amplifies the most the buoy's motion, as can be seen in the graph 1.3.

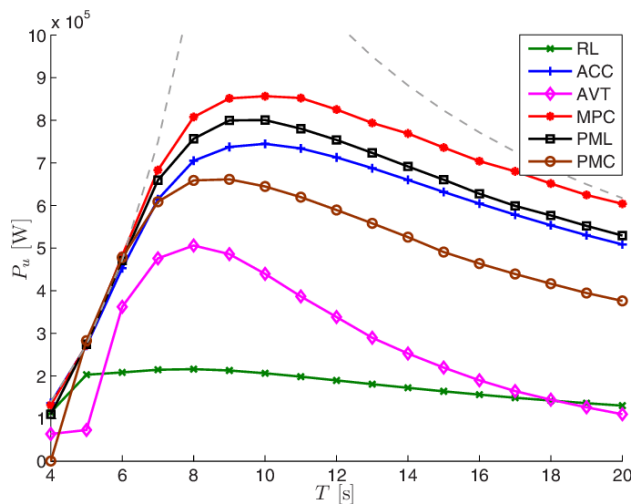


**Figure 1.3:** Budal diagram showing the average absorbed power for the different control strategies with varying wave period. The incident waves were regular with height  $H=3$  m. (PML=Latching RL=Passive damping

ACC=Approximate complex-conjugate  
 PMC=Declutching  
 AVT=Approximate optimal velocity  
 MPC=Model predictive control) [7]

Latching control strategy can be integrated with the Declutching technique, which is designed to temporarily reduce damping to accelerate the buoy's motion, by interrupting power absorption, being very effective especially when the natural frequency is lower than the wave's one. [4]. By combining these two approaches, a substantial enhancement in energy absorption is achieved across a broad spectrum, as visually depicted in the Figure 1.4.

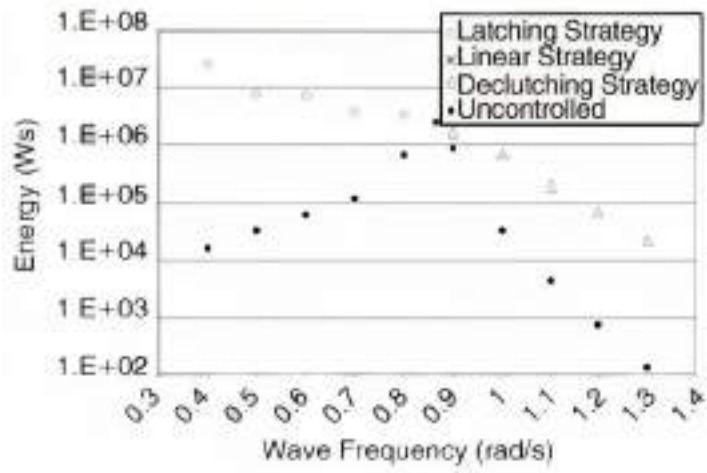


**Figure 1.4:** Energy absorption spectrum width enhancement thanks to Latching and Declutching control [4]

## Contents of this chapter

---

2.1	Hardware . . . . .	10
2.1.1	Tank . . . . .	11
2.1.2	Beach . . . . .	11
2.1.3	Wave generator . . . . .	12
2.1.4	WEC . . . . .	13
2.1.5	Micro controller and electronic . . . . .	15
2.1.6	Wave probe . . . . .	16
2.2	Software and control strategy . . . . .	17
2.2.1	Modified latching . . . . .	17
2.3	Rig pictures . . . . .	19

---

## 2.1 Hardware

In light of the preceding deliberations, a comprehensive inventory of components satisfying the stipulated criteria has been compiled, subsequently substantiated with 3D technical representation.

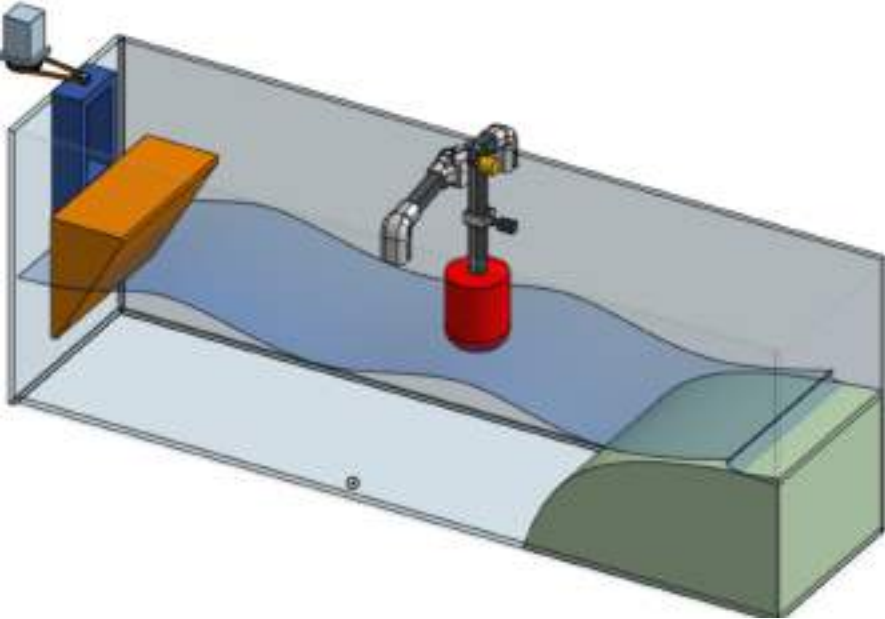
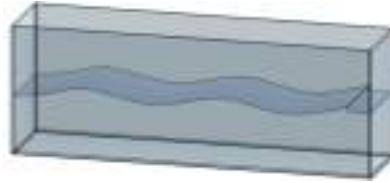


**Figure 2.1:** Picture of the complete setup

### 2.1.1 Tank

The tank's design has been tailored to facilitate convenient transportation within vehicles such as cars or standard-sized elevators, thereby ensuring its portability as necessitated by the circumstances. Simultaneously, the tank's dimensions are calibrated to maintain a balance between practicality and the generation of optimal wave conditions [8].



In order to get the tank dimension the wavelength is calculated [8] as

$$\lambda = \frac{gT^2}{2\pi} \sqrt{\frac{\tanh(4\pi^2d)}{T^2g}} \quad (2.1)$$

with  $d$  being the water depth and  $T$  the desired maximum period. The length of the tank has been obtained, as a rule of thumb, as  $L = 3\lambda$ , a good balance between a good wave development and saving space. In order to obtain deep water waves be sure to have  $d > \lambda/2$  [8]. Embracing the configuration of a flume tank, the tank's width has been judiciously minimized to conserve both space and weight, thereby optimizing the overall system design.

To streamline calculations a MATLAB script has been developed.

Acrylic material emerged as the most suitable choice, primarily attributed to its ease of manipulation, remarkable durability, and exceptional transparency characteristics.

Dimension: L 1300 × D 450 × W 300 mm | Material: 10mm acrylic sheets

### 2.1.2 Beach

To effectively mitigate the occurrence of reflective waves, the implementation of a wave-damping structure at the terminus of the tank is imperative. Literature exploration culminated in the determination that a slope of  $6^\circ$  at the water's surface,



at the water's surface,

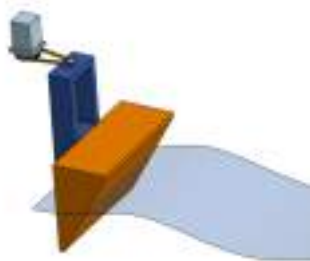
a beach length spanning at least one wavelength, and an elevation surpassing the water surface level are prerequisites for optimal performance[9].

In an endeavor to curtail weight while retaining structural integrity, the beach is fashioned from acrylic sheets and hermetically sealed, allowing air to fill the enclosed volume and achieving a substantial reduction in weight, exceeding 30 kilograms.

Additionally, a highly porous mesh overlay is deployed atop the structure to forestall the propagation of high-frequency waves, further contributing to the proficiency of the wave-damping system.

### 2.1.3 Wave generator

An integral component of paramount significance is the Wave Maker. Within this realm, two primary methodologies exist for wave generation. Notably, the flap type method stands out for its superior wave quality and amplitude. However, it necessitates a sealed connection with



the tank to ensure electronic components remain dry, a requirement that occupies considerable space, and demands higher energy input to propel the water effectively. Consequently, a wedge configuration has been adopted as the most pragmatic approach, effectively reconciling practicality, space-saving considerations, and operational efficiency within the constraints of the system design [10][11].

The system is orchestrated around a stepper motor, a choice rooted in its ease of control and robust torque capabilities. To achieve the transformation from rotational to linear motion, a screw-ball rail is employed, synergizing with the motor's operation to yield a remarkable degree of movement precision. To align with the stipulated speed requisites, a pulley system has been incorporated.

The wedge movements has been programmed to be as close as possible to a sinusoidal motion.

### 2.1.3.1 Datasheet

Piece	Specifications
Stepper motor	Neema 23 4.2A Bipolar (23HS45-4204S)
Linear rail	L: 200mm Peace: 8mm Stroke: 122.85 (Z axis 3D printer 4080U)
Pulley system	Aluminum pulley 80T and 20T Hole: 8mm Belt: 250-2GT
Motor controller	Bipolar controller Peak: 4.2A (Dir Pul control) (DM542)

**Table 2.1:** Wave maker datasheet

### 2.1.4 WEC

The WEC is a composite assembly comprising a gantry and a buoy. Constructed from aluminum extrusion bars, 3D printed joints, and equipped with wheels and bearings, the gantry has a dual purpose. It is designed to confine the motion predominantly to a singular DoF, while concurrently facilitating the vertical oscillation of the buoy with minimal frictional resistance.



The buoy itself is fashioned from High-Density Expanded Polystyrene (HD EPS) material to ensure buoyancy, supplemented by an aluminum bar to interface with the gate.

Notably, as can be seen in Figure 1.4, the Latching control is very effective for incoming wave with frequency lower than the natural frequency of the device, so the floating body has been designed with a natural frequency significantly higher than that of the propagating waves, thereby enhancing the discernibility of control effectiveness [4]. Because of the uncertainty or impossibility to get frictional and viscous forces of the complete model, considering also the small impact of them at such small scale, to obtain the dimension of the buoy the model (1.1) has been simplify to a spring-mass-damper system.

The model thus turns out to be

$$\ddot{x}m + 2\zeta\omega_n\dot{x} + \omega_n^2x = f_{ext} \quad (2.2)$$

Where  $x$  is displacement,  $\zeta$  is the damping coefficient estimated from simulation,  $f_{ext}$  are external forces and  $\omega_n$  is the natural frequency, calculated as

$$\omega_n = \sqrt{\frac{k}{m}} \quad (2.3)$$

where  $k$  is the buoyancy force over the displacements and  $m$  is the sum of the total suspended mass and the infinity added mass  $m_{add}$  of a semi-sphere.

By fixing  $\omega_n$  around 0.1-0.2 s has been possible to obtain the dimension and mass of the floating body. The  $\omega_n$  has been chosen so low to ensure compliance for additional friction forces. Those friction forces will result in a real resonating frequency  $\omega_d$  a bit slower than  $\omega_n$  that can be computed as

$$\omega_d = \omega_n\sqrt{1 - \zeta^2} \quad (2.4)$$

To streamline calculations a MATLAB script has been developed.

#### 2.1.4.1 Datasheet

Piece	Specifications
Buoy	Diameter: 95mm Total height:120mm 2020 Aluminum bar extrusion and 3Dprinted mount
Gantry	2020 Aluminum bar extrusion 3D printed press-fit joints Vshape 3D printer wheels gate with bearings

**Table 2.2:** WEC datasheet

### 2.1.5 Micro controller and electronic

A solenoid has been selected as the preferred locking mechanism, primarily due to its rapid response, imperative due to the time constant of the system being in the order of hundreds of milliseconds, and straightforward controllability, with just a simple Transistor and a small circuit.



For power generation, a Lego motor was employed as the prime candidate, offering commendable power output in the context of low amplitude motions. To tailor its suitability to the system, the motor underwent alterations in terms of gear ratio, by reducing it to decrease the damping effect and lowering the torque required to spin it. The modified motor was subsequently encased within a 3D printed shell and spring tense to ensure a good contact.

A total of three Arduino UNO boards were employed. The first board orchestrates Wave Maker control, effectively interfacing with the motor controller via the PUL and DIR pins. The second board is tasked with precise activation of the solenoid mechanism, adhering to predetermined timing intervals. The third board assumes responsibility for power output measurement and real-time data visualization.



To facilitate comprehensive data acquisition encompassing both device dynamics and wave characteristics, a dedicated data acquisition system was devised utilizing an additional Arduino Uno board. This system incorporates distinct sensors and probes, including a Time-of-Flight (TOF) sensor to capture buoy position and velocity, a specially crafted wave probe to gauge wave properties, and the means to measure the power output generated by the motor.



### 2.1.5.1 Datasheet

Piece	Specifications
Micro controller	Arduino UNO
Servo motor	Micro servo 9g
Solenoid	Force: 5N Stroke: 10mm push pull (HS-0530B DC6V)
Motor	LEGO motor 9V DC Mini-Motor (71427c01)
Transistor	Transistor Darlington
Position sensor	TOF sensor (VL6180X)

**Table 2.3:** Electronic datasheet

### 2.1.5.2 Circuit

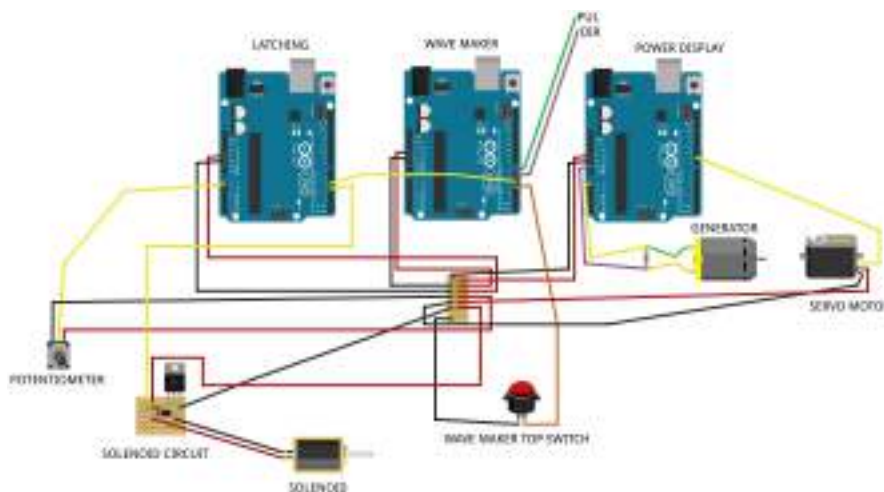


**Figure 2.2:** Electronic circuit of the plant

### 2.1.6 Wave probe

To facilitate wave measurements, a capacitance-based probe was designed and developed. The probe capitalizes on the modulation of capacitance resulting from the immersion of its two armatures in water. Notably, the observed variation in capacitance serves as a direct proxy for changes in the water surface level, rendering the probe an effective tool for capturing wave characteristics.

Commonly, the operation of probes necessitates the incorporation of intricate and specialized electronics. However, to integrate the probe within the Arduino platform, the Touch Sensor library has been adeptly employed. This strategic implementation facilitates real-time

measurement of capacitance values, allowing to capture relevant data using the Arduino system.

A dedicated calibration procedure was instituted, involving the acquisition of three distinct capacitance values corresponding to stationary water levels at 2, -2, and 0 cm. These values were subsequently employed to execute a linear interpolation procedure, effectively establishing a correlation between capacitance values and positional variations.

The probe can be entirely 3D printed and requires just two aluminum sheets and a 1.5 M $\Omega$  trimmer.

## 2.2 Software and control strategy

### 2.2.1 Modified latching

Owing to the exceedingly brief wave periods, the real-time control implementation has posed significant challenges. Notably, accommodating the latching time, which is on the order of hundred milliseconds, with a requisite precision in the order 10 milliseconds, has proven intricate. To attain feasibility, a revised rendition of the latching profile has been devised. This adaptation affords greater tolerance in timing by extending the latching duration, albeit triggered only once per wave period. The outcome of this modification ensures that the buoy's velocity aligns with the excitation force exclusively during the rising edge of the wave. Following this phase, the buoy is released to undergo free-fall motion. The biggest advantage of this revision is that it make possible to calculate the timing just once at the beginning of every cycle, also with more compliance, while for the "normal" latching (Figure ??) the time intervals are doubled for every cycle, leading to a summation of double the possible errors and to an even faster timing intervals.

Given the constrained time-frame, the latching operation is synchronized with the wedge motion, thereby minimizing potential discrepancies. Additionally, a user-adjustable knob facilitates the manipulation of latching time, fostering user interaction and real-time observation of the control's impact, which supposed to be strongly dependent on the timing, being able to lead to really damped behave if wrong.



A rough esteem of the optimal latching time has been obtained as

$$T_L = T_W - T_N \quad (2.5)$$

where  $T_N$  is the natural oscillation period of the floating body and  $T_W$  is the period of incoming waves. Then further adjustment has been made to make fine correction of  $T_L$  by trying to maximize the power output.

## 2.3 Rig pictures

Here are Figure 2.3 and 2.4 which show all the components cited above assembled.

From the pictures it can be seen that the setup follows the 3D drawings, apart from some little exception due to last minutes modifications.

In Figure 2.4 the two power supply of 5V and 36V are visible in the low right corner, which are responsible of powering the Arduinos and solenoid and the stepper motor respectively.

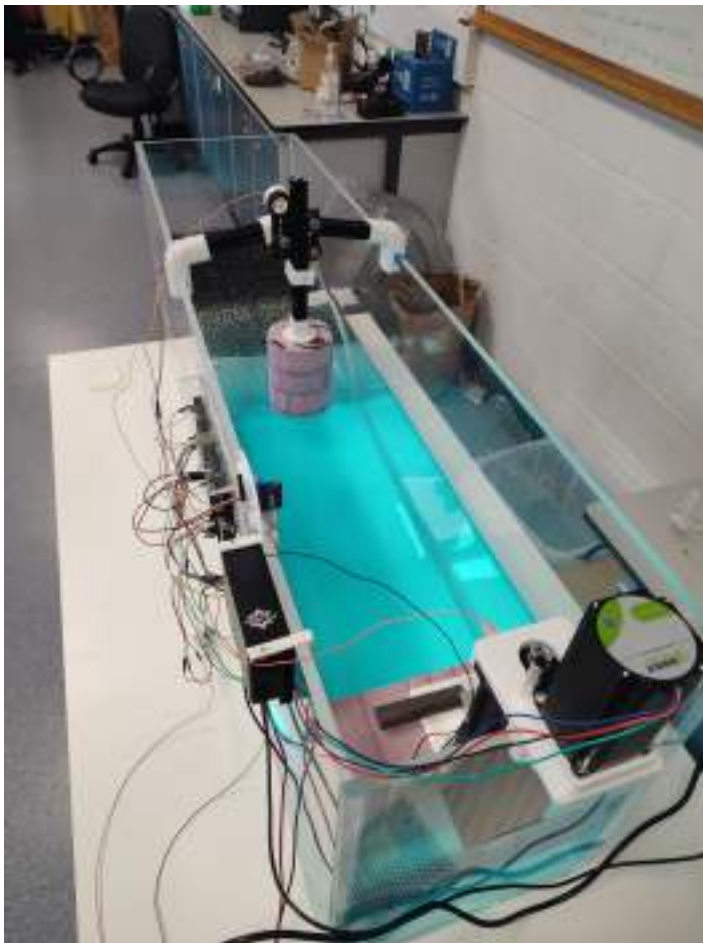


**Figure 2.3:** Picture of the complete setup. The water has been dyed to improve the visual effect



**Figure 2.4:** Picture of the complete setup

## Contents of this chapter

---

3.1	Wave fidelity . . . . .	21
3.2	Phase regulation . . . . .	23
3.3	Power increase . . . . .	24

---

To ensure precise measurements, the experimental setup was relocated to the Dundalk Institute of Technology, where the integration of specialized, professional-grade wave probes was facilitated. Specifically, resistive probes were employed to accomplish the data acquisition process for the wave maker (WM).

Measurements were conducted at the intended position for the WEC, specifically positioned at approximately one-third of the total length from the beach. The WM underwent testing with various wave frequencies and motion amplitudes. From these tests, a frequency of approximately 0.86 seconds per period was determined to be the optimal compromise between wave quality, visual impact, and control time constant feasibility. Higher frequency waves, although visually appealing, would have posed challenges for control, by diminishing the time constant. Conversely, lower frequency waves, while easier to manage, would have been incompatible with the tank's dimensions.

All subsequent tests on the WEC were conducted using the same selected frequency and amplitude.

### 3.1 Wave fidelity

As can be seen in Figure 3.1 the wave amplitude measures around 2 cm PP. Notably, a marginal offset of approximately 2 mm is discernible, possibly attributed to the elevated buoyancy of the wedge, thereby resulting in an accelerated upward movement during its trajectory.

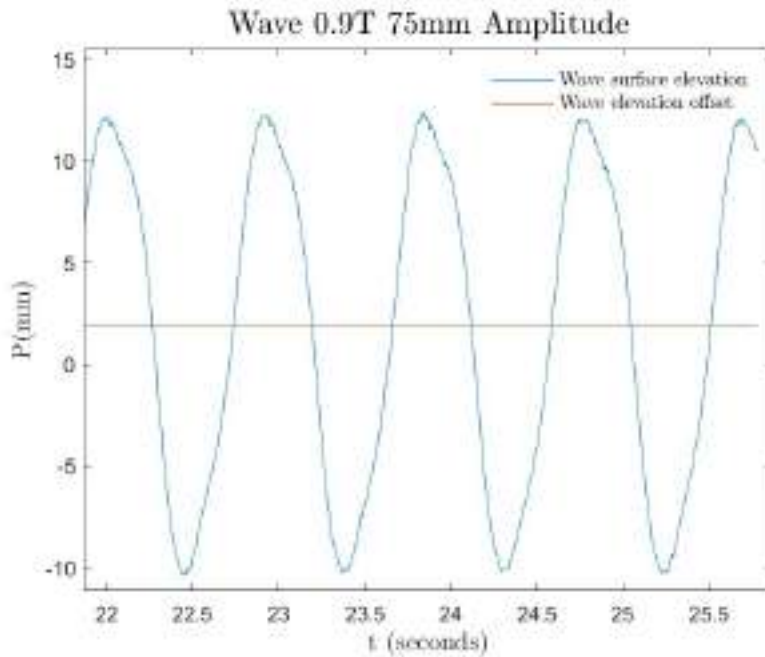


**Figure 3.1:** Snippet of the wave profile

As can be seen in Figure 3.2, the Fourier transform analysis reveals a pronounced peak near the desired frequency of 0.125 Hz. The analysis further illustrates a scarcity of significant harmonics, with the highest occurrence observed approximately three times the principal frequency. This phenomenon can be attributed to the dimensions of the tank, which, interestingly, align three times with the wavelength, thus influencing the harmonics' manifestation.

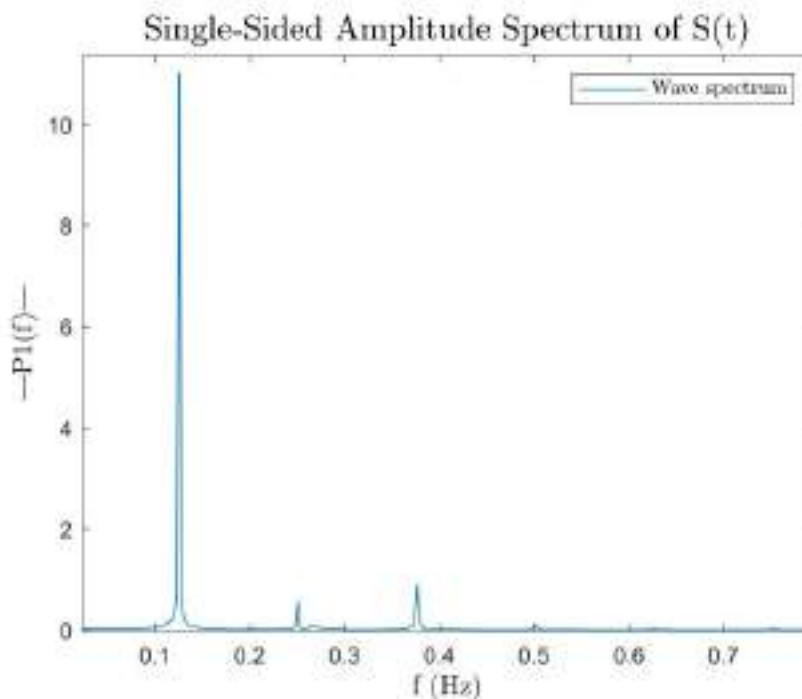


**Figure 3.2:** Fourier transform of the data with same wedge movement

## 3.2 Phase regulation

As previously mentioned, the fundamental principle underlying the latching control is phase regulation [12]. Achieving an amplified motion necessitates the activation of the solenoid with remarkable precision, especially given the exceedingly short time constant arising from the wave period.

The provided Figure 3.3 illustrate this concept. The discernible phase shift in the velocity profile becomes evident upon comparison with the free-motion curve. Notably, in the provided graph, it becomes apparent that the negative slope of the latched velocity profile aligns with the corresponding counterpart of the excitation force.

Due to the modifications implemented in the control profile, as detailed in the preceding section, only half of the cycle demonstrates phase alignment.

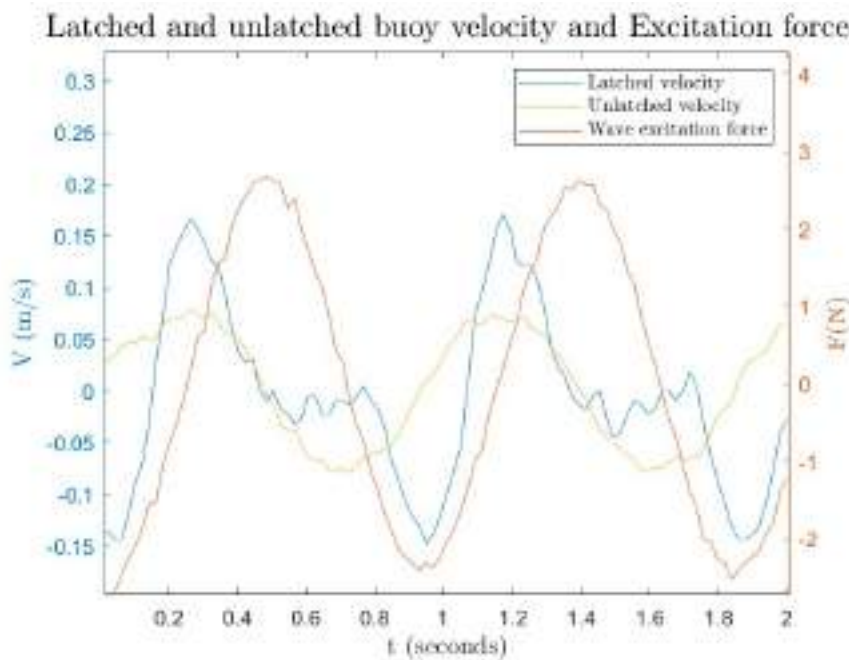


**Figure 3.3:** Latched and unlatched velocity profile in relation with wave excitation force

As a consequence, discernible amplification in the buoy's amplitude is readily apparent in Figure 3.4 and Figure 3.5, effectively highlighting the successful implementation and efficacy of the control action.

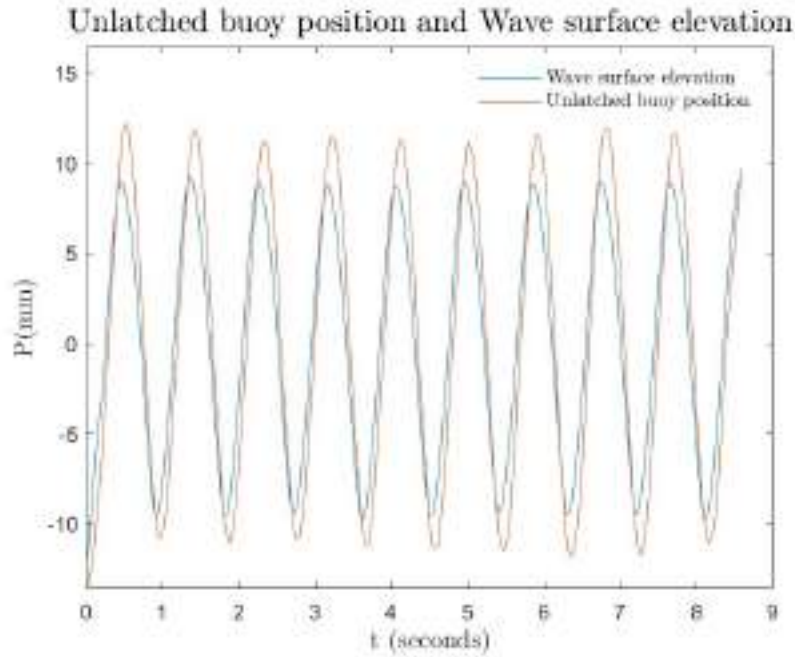


**Figure 3.4:** Buoy position in relation with water surface level with Latching control inactivated

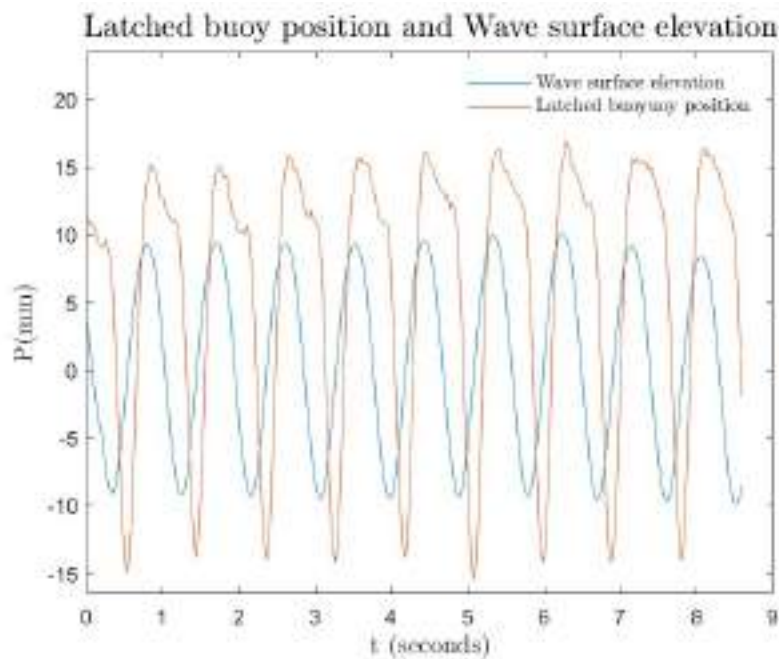


**Figure 3.5:** Buoy position in relation with water surface level with Latching control activated

### 3.3 Power increase

Assessing the comprehensive enhancement of the system's performance finds a reliable benchmark in the power extracted from the PTO mechanism. The Figure 3.6 display power measurements of the motor output, acquired using a fixed resistor of  $464 \Omega$ .

For presentation purposes, only the positive wave segment is shown, as the Arduino's Analog port solely reads positive voltage values. Incorporating a rectifier would have been advantageous to harness the entirety of available power; however, the constrained voltage output remains inadequate to surpass the typical threshold voltage of common diodes.

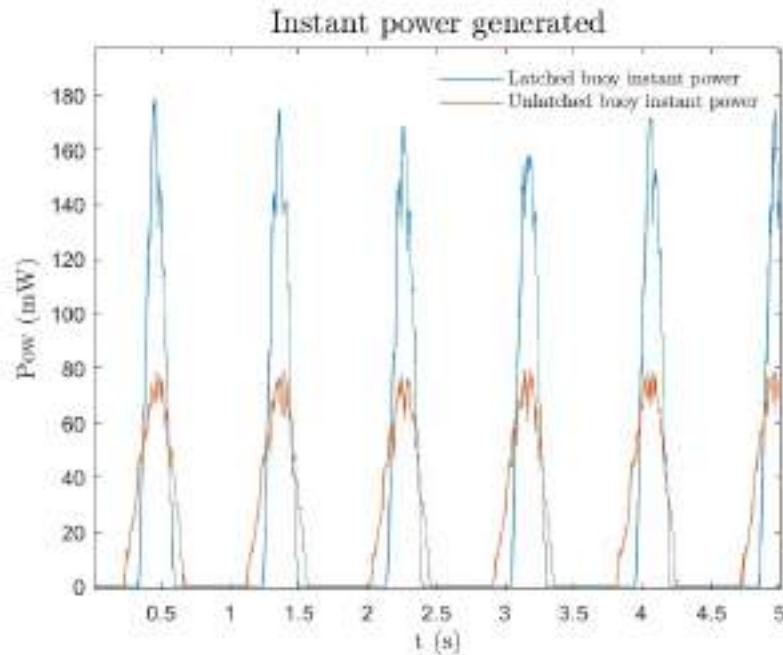


**Figure 3.6:** Instant power generated (just positive semi-wave)

The graph readily illustrates the discernible contrast between uncontrolled and controlled motion in terms of power generation, where its easy to see an increase of over 100% in the peak power.

The energy generated within a 5-second interval was computed, yielding 39.46 mWh for the buoy in free motion and 52.05 mWh for the controlled motion scenario. This signifies a notable increase of 32% in energy production.

The project has successfully achieved all the objectives outlined at its inception. The tank has emerged as a powerful educational tool, capable of engaging a diverse audience, ranging from university students to young elementary school pupils, to adults with or without engineering background. Its compelling visual impact and the user-friendly adjustment of latching times via a simple knob make it accessible and interactive.

Furthermore, the data collected demonstrates a notable correlation between the anticipated sinusoidal wave behavior and the observed results, as well as the buoy's responsive performance. These attributes position the rig as a valuable resource for low-level developmental projects. In this context, the incorporation of multiple sensors for wave measurement, buoy movement tracking, and power assessment plays a pivotal role in enhancing its capabilities.

The path leading to the attainment of the final results and the accompanying challenges have been intellectually stimulating, closely resembling those encountered during the construction of significantly larger and more complex tanks. Every aspect of this endeavor has been documented, and comprehensive resources, including 3D drawings and Arduino code, will be made readily available. This resourcefulness enables educational institutions to gain firsthand experience with wave energy experimentation, fostering a deeper understanding of the subject matter.

# Bibliography

- [1] J. Xie and L. Zuo. 'Dynamics and control of ocean wave energy converters'. In: *International Journal of Dynamics and Control* 1 (3 Sept. 2013), pp. 262–276. DOI: [10.1007/s40435-013-0025-x](https://doi.org/10.1007/s40435-013-0025-x) (cited on pages 2–4, 6).
- [2] M. D. Esteban. 'Classification of Wave Energy Converters'. In: *Recent Advances in Petrochemical Science* 2 (4 Aug. 2017). DOI: [10.19080/RAPSCI.2017.02.555593](https://doi.org/10.19080/RAPSCI.2017.02.555593) (cited on pages 2, 4).
- [3] G. Bacelli, R. Genest, and J. Ringwood. 'Nonlinear control of flap-type wave energy converter with a non-ideal power take-off system'. In: *Annual Reviews in Control* 40 (2015), pp. 116–126. DOI: [10.1016/j.arcontrol.2015.09.006](https://doi.org/10.1016/j.arcontrol.2015.09.006) (cited on page 3).
- [4] 'Energy-Maximizing Control of Wave-Energy Converters: The Development of Control System Technology to Optimize Their Operation'. In: *IEEE Control Systems* 34 (5 Oct. 2014), pp. 30–55. DOI: [10.1109/MCS.2014.2333253](https://doi.org/10.1109/MCS.2014.2333253) (cited on pages 5–9, 13).
- [5] G. Bacelli. 'Optimal control of wave energy converters' (cited on page 7).
- [6] C. Windt et al. 'Reactive control of wave energy devices – the modelling paradox'. In: *Applied Ocean Research* 109 (Apr. 2021), p. 102574. DOI: [10.1016/j.apor.2021.102574](https://doi.org/10.1016/j.apor.2021.102574) (cited on page 7).
- [7] J. Hals, J. Falnes, and T. Moan. 'A Comparison of Selected Strategies for Adaptive Control of Wave Energy Converters'. In: *Journal of Offshore Mechanics and Arctic Engineering* 133 (3 Aug. 2011). DOI: [10.1115/1.4002735](https://doi.org/10.1115/1.4002735) (cited on page 8).
- [8] M. I. T. Ocean-engineering. *Water Waves* (cited on page 11).
- [9] Edimburg-Design. *Wave tank builders* (cited on page 12).
- [10] A. H. Nikseresht and H. B. Bingham. 'A Numerical Investigation of Gap and Shape Effects on a 2D Plunger-Type Wave Maker'. In: *Journal of Marine Science and Application* 19 (1 Mar. 2020), pp. 101–115. DOI: [10.1007/s11804-020-00135-5](https://doi.org/10.1007/s11804-020-00135-5) (cited on page 12).
- [11] B. Sun et al. 'A simplified method and numerical simulation for wedge-shaped plunger wavemaker'. In: *Ocean Engineering* 241 (Dec. 2021), p. 110023. DOI: [10.1016/j.oceaneng.2021.110023](https://doi.org/10.1016/j.oceaneng.2021.110023) (cited on page 12).
- [12] G. Giorgi and J. V. Ringwood. 'Implementation of Latching Control in a Numerical Wave Tank'. In: () (cited on page 23).